

MAGNETIC RESPONSE AND NEGATIVE REFRACTION AT OPTICAL FREQUENCIES ON THE BASIS OF ELECTRONIC TRANSITIONS IN RARE-EARTH IONS DOPED CRYSTALS

Xiaojian Fu¹, Yuanda Xu², and Ji Zhou^{1, *}

¹State Key Laboratory of New Ceramics and Fine Processing, Department of Materials Science and Engineering, Tsinghua University, Beijing 100084, China

²School of Physics, Peking University, Beijing 100871, China

Abstract—Magnetic response based on a two-level magnetic dipole transition in rare earth ions doped crystals was studied. Semi-classic theory and Wigner-Eckart theorem were used to calculate the magnetic permeability. It is found that negative permeability can be attained near the transition frequencies. In order to realize simultaneously negative permittivity and negative permeability, an electric dipole transition at the same frequency was also adopted, and a negative refraction region with a bandwidth of 0.57 MHz is demonstrated in $(\text{Yb}_{0.02}\text{Sm}_{0.02}\text{Y}_{0.96})_3\text{Al}_5\text{O}_{12}$ crystal. This explores a new route to obtain magnetic response and negative refraction at optical frequencies with nature-existed materials instead of metamaterials.

1. INTRODUCTION

Artificially engineered electromagnetic (EM) structures, so called metamaterials, provide a route to create new materials with unprecedented electromagnetic properties and new prospects for manipulating EM wave [1–6]. Metamaterials were first demonstrated for microwave frequencies [7, 8], but it has been challenging to build three dimensional one for optical frequencies, especially in visible region, because of nanofabrication limitation, mesoscopic physics problem, and strong energy dissipation in metals [9–11].

Well-used structure unit for metamaterials are sub-wavelength components with electric and magnetic dipole resonance, such as split

Received 7 December 2012, Accepted 28 February 2013, Scheduled 28 February 2013

* Corresponding author: Ji Zhou (zhouji@tsinghua.edu.cn).

ring resonator (SRR) and derivatives [8,12]. Such structures are analogous to atoms while they interact with EM wave. Whereas, to break the limitation of optical metamaterials, electron transition between energy levels in atoms might be a useful alternative as a unit to achieve EM resonance in visible optical region [13]. A mechanism on the basis of electric and magnetic dipole transitions in gas media was proposed recently [14,15]. However, compared to electric dipolar oscillator, magnetic dipolar oscillator in most atoms is much weaker, so direct magnetic transition is usually omitted. In order to obtain simultaneously negative permittivity and permeability, multi-level model and quantum coherence method are adopted to generate effective magnetic transition [16], however, an additional beam present besides the signal or probe beam should be required to keep the state of coherence, so the complexity of system is added. Based on quantum optics methods, the possibility of realizing negative refraction in doped semiconductors has also been investigated [17,18]. The coherent electric dipole and magnetic dipole transitions in the hydrogen-like dopant atom response to the probe light and generate the negative permittivity and permeability, respectively.

Rare-earth ions in solids supply a special system for the electric and magnetic dipole transitions. In general, the electric dipole (ED) transitions between the states of $4f$ electronic configurations of an isolated rare-earth ion are forbidden by the parity selection rules, however, the magnetic dipole (MD) transitions between of $4f$ states are allowed [19]. Rare earth ions with plenty of energy levels possess relatively strong magnetic dipole oscillator. The electric-dipole transitions become partly allowed if odd-order terms in the expansion of the static or dynamic crystalline-field potential admix states of higher and odd-parity configurations into $4f$ [20]. So it is possible to keep the strength of electric and magnetic dipole transitions in a similar level. A left-handed property of Er-doped crystal was demonstrated in a finite domain of parameters, however, the general theoretical feasibility is under investigation [21, 22].

In this paper, f - f MD transition in rare-earth doped crystals is investigated and general expressions of magnetic permeability are derived according to semi-classic theory and Wigner-Eckart theorem. As an example, the EM parameters of Sm^{3+} and Yb^{3+} co-doped $\text{Y}_3\text{Al}_5\text{O}_{12}$ (abbreviated as YAG) crystal are calculated numerically, and a frequency band with negative refractive index is observed. As compared to the previous works, two-level scheme in condensed matter and weak field condition are designed, which simplify the model to a large extent.

2. MAGNETIC DIPOLE TRANSITION

Let us consider the electronic resonant transition between an excited state $|1\rangle$ and the ground state $|2\rangle$, as shown in Fig. 1. According to selection rules, the same parity of the two states suggests magnetic dipole transition is allowed. Excited by a weak enough light, in semi-classical theory, the density matrix element related to magnetization has the following form [23, 24]:

$$\rho_{12} = \frac{-i}{\hbar} \mu_{12} B \frac{\rho_{11} - \rho_{22}}{i\Delta + \gamma} \quad (1)$$

where μ_{12} and B are magnetic dipole matrix element and the amplitude of magnetic component of probe light, respectively. Under Maxwell-Boltzmann distribution, the density matrix elements ρ_{11} and ρ_{22} are set to be 0 and 1, respectively. Δ is frequency detuning with the form of $\Delta = \omega_0 - \omega$, where ω_0 is the resonant transition frequency of the two-level system and ω is the angular frequency of the probe light. γ is the average of γ_1 and γ_2 , which represent the decay rates of level $|1\rangle$ and level $|2\rangle$, respectively.

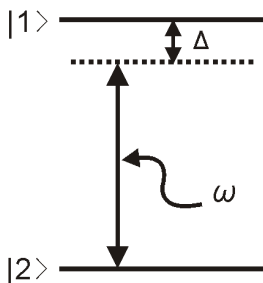


Figure 1. The scheme of two-level electronic resonant transition under a weak probe field, where ω is the angular frequency of probe light, and frequency detuning Δ is the difference between the transition frequency ω_0 and ω .

By denoting that $m = \rho_{12}\mu_{21}$ and $m = \mu_0\alpha_m B$, we find the atomic magnetic susceptibility has the following expression

$$\alpha_m = \frac{-i}{\mu_0\hbar} |\mu_{21}|^2 \frac{\rho_{11} - \rho_{22}}{i\Delta + \gamma} \quad (2)$$

Here, m is the magnetization of a single atom or ion, and μ_0 is the permeability of vacuum.

Since the host crystal does not response to the magnetic field, the relative magnetic permeability in Gauss units can be written as

$$\mu_r = 1 / (1 - 4\pi N\alpha_m) \quad (3)$$

Now, let us deduce the expression of the magnetic dipole matrix element μ_{21} . In the case of $4f$ electrons of rare earth ions, the initial and the final states have the state functions of $|4f^N SLMJ\rangle$ and $|4f^N S'L'M'J'\rangle$, respectively, where N is the number of $4f$ electrons, S , L and J are the spin, orbital and total angular moments, M is the projection of J on the z axis. Using the Wigner-Eckart theorem [25], we can get

$$\mu_{21} = (-1)^{J+M} \frac{e\hbar}{2mc} \begin{pmatrix} J & 1 & J' \\ -M & q & M' \end{pmatrix} \langle 4f^N SLMJ || L + 2S || 4f^N S'L'M'J' \rangle \quad (4)$$

For magnetic dipole transition, $\Delta S = 0$, $\Delta L = 0$, and if $J' = J - 1$, the reduced matrix element can be calculated as follows.

$$\begin{aligned} & \langle 4f^N SLMJ || L + 2S || 4f^N S'L'M'J' \rangle \\ &= [(S+L+J+1)(S+L-J+1)(S-L+J)(-S+L+J)/4J]^{1/2} \quad (5) \end{aligned}$$

With Eqs. (3), (4) and (5), the magnetic permeability near the transition frequency in rare earth doped crystal can be calculated. As a typical example, here we analyze the magnetic response in Yb : YAG crystal with the component of $(\text{Yb}_x\text{Y}_{1-x})_3\text{Al}_5\text{O}_{12}$. YAG with the cubic symmetry has isotropic optical properties and excellent physical and chemical features, and therefore it is widely used as the host crystal of solid state lasers [26]. Rare earth ions, from Ce^{3+} to Yb^{3+} , possess especial electronic structure and abundant energy levels, so relatively strong MD transition is not difficult to find. In Yb^{3+} , the $4f^{13}$ electron configuration has only two energy-level manifolds, the ground state ${}^2\text{F}_{7/2}$ and an excited state ${}^2\text{F}_{5/2}$, which are separated by about 10600 cm^{-1} [27]. According to selection rules, MD transition is allowed between them. It is assumed that $M = M' = 1/2$ and $q = 0$. The magnitude of γ_{12} is about 10^5 Hz .

The numerical results are presented at Fig. 2. In order to investigate the effect of dopant concentration on magnetic response, we design three values of Yb^{3+} content, which are $x = 0.01$, 0.02 and 0.05 . It is found that the permeability shows an obvious resonance characteristic near the transition frequency and abnormal magnetic response is obtained in the resonant range, especially the high-frequency part. With the increase of Yb^{3+} concentration, the resonant frequency exhibits a red shift, the resonant region gets wider and the amplitude becomes larger according to Fig. 2(a). Fig. 2(b) shows that the imaginary part of permeability increases obviously with the increasing x value. Now, let us take the crystal $x = 0.02$ for example to discuss the magnetic resonant behavior in detail. From the detuning

frequency of -10 MHz, the real part of permeability (μ_r) becomes less than one, and comes to be negative from 0.04 MHz, and hence the bandwidth for negative permeability is 0.66 MHz. The imaginary part (μ_i) which is related to attenuation arrives at a maximum of 6.95 at the detuning frequency of 0.70 MHz. Far from this point, μ_i reduces quickly to zero. In addition, the minimum of μ_r reaches -2.47 with the μ_i of 3.56 .

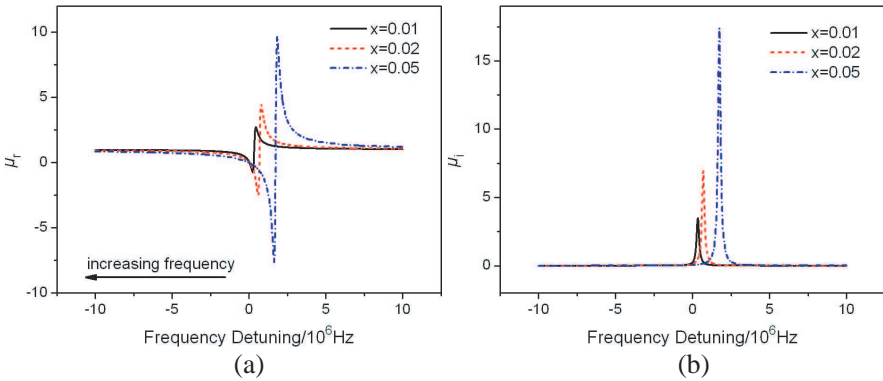


Figure 2. The relation between magnetic permeability of $(Yb_xY_{1-x})_3Al_5O_{12}$ crystal and frequency detuning. (a) μ_r , real part of magnetic permeability. (b) μ_i , imaginary part of magnetic permeability. The concentrations of Yb^{3+} ion are $x = 0.01, 0.02$ and 0.05 respectively.

3. NEGATIVE REFRACTION BEHAVIOR

A two-level system with opposite parity can also be investigated by this method. The key idea is to use reduced matrix element $U(\lambda)$ and oscillator strength $\Omega(\lambda)$ to describe the electric dipole matrix element \wp_{12} . According to Judd-Ofelt theory [28–30], we have

$$|\langle 4f^N JM | D_q^1 | 4f^N J' M' \rangle|^2 = \frac{1}{3(2J+1)} \sum_{\lambda=2,4,6} \Omega_\lambda U(\lambda) \quad (6)$$

where D_q^1 is a component of the electric dipolar operator corresponding to the transition from the ground state $|2\rangle$ to the excited state $|1\rangle$.

Considering $\wp_{12} = e|\langle 4f^N JM | D_q^1 | 4f^N J' M' \rangle|$, we can get

$$\wp_{12} = \frac{e}{\sqrt{3(2J+1)}} \sqrt{\sum_{\lambda=2,4,6} \Omega_\lambda U(\lambda)} \quad (7)$$

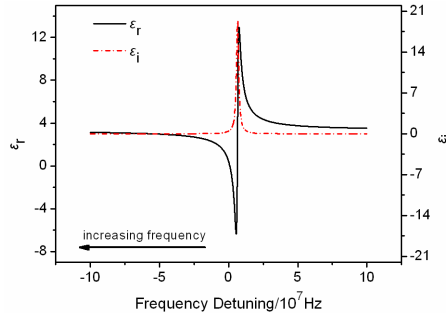


Figure 3. The frequency-dependent dielectric function curves. ε_r and ε_i represent real part and imaginary part of permittivity, respectively.

For the ED transition, the expression of atomic polarizability is similar with Eq. (2), which is given by

$$\alpha_e = -\frac{i}{\varepsilon_0 \hbar} |\rho_{12}|^2 \frac{\rho_{11} - \rho_{22}}{i\Delta + \gamma_{12}} \quad (8)$$

Finally, by combining Eqs. (7) and (8) we can easily get the atomic polarizability of rare-earth ions in crystal, and hence, considering the local field correction, the relative permittivity according to Clausius-Mossotti relation [31] in SI units could be described by

$$\chi_e = \varepsilon_c + N\alpha_e \left(1 - \frac{N\alpha_e}{3}\right)^{-1} \quad (9)$$

where ε_c is the relative permittivity of the host crystal.

Here, we use the transition between ${}^6H_{5/2}$ and ${}^6F_{11/2}$ in Sm^{3+} in order to realize electric dipole resonance at the same frequency with magnetic resonance. The following electric dipole parameters $\Omega_\lambda(\lambda = 2) = 1.20 \times 10^{-24}/\text{m}^2$, $\Omega_\lambda(\lambda = 4) = 2.08 \times 10^{-24}/\text{m}^2$, $\Omega_\lambda(\lambda = 6) = 1.72 \times 10^{-24}/\text{m}^2$, $U(2) = 0$, $U(4) = 0.001$, and $U(6) = 0.052$ are adopted [32, 33]. The magnitude of γ_{12} is set to be 10^6 Hz. ε_c is about 3.31 with a negligible imaginary part [34].

Figure 3 shows the curve of dielectric function of YAG crystal with 2% Sm^{3+} . Similar resonance behavior is also observed near the electronic transition frequency and abnormal dielectric response is obtained in the resonant range. When frequency detuning is between 0.01×10^7 Hz and 0.63×10^7 Hz, the real parts of dielectric function are negative, and its bandwidth is 6.2 MHz. The minimum of real part is -6.34 with an imaginary part of 9.61.

As previously mentioned, rare earth ions doped crystal can realize simultaneously ED and MD resonances at optical frequencies, and the strength of two kinds of oscillators are of the similar order of

magnitude if appropriate ions and their concentrations are exploited. Therefore, negative refraction can be obtained at the frequency region with both negative permittivity and magnetic permeability. The underlying requirement is that the ED and MD transitions can be excited by one probe light (the uniform frequency and wave vector direction). And then the induced moments can be $\mathbf{e} // \mathbf{E}$ and $\boldsymbol{\mu} // \mathbf{B}$, where \mathbf{e} and $\boldsymbol{\mu}$ are the ED and MD moments, respectively, and \mathbf{E} and \mathbf{B} correspond to electric field and magnetic field. Thus the electric response is perpendicular to the magnetic response, which makes the left-handed property possible. In order to satisfy this condition, the two sets of two-level transitions should be selected according to the selection rules under a certain crystal since the crystal symmetry plays a role in determining the transition probabilities [13]. In this work, we take the Yb and Sm co-doped YAG crystal as an example, in which simultaneous magnetic and electric dipolar resonances can be achieved around 10600 cm^{-1} and negative refraction is observed near that frequency as shown in Fig. 4. In $(\text{Yb}_{0.02}\text{Sm}_{0.02}\text{Y}_{0.96})_3\text{Al}_5\text{O}_{12}$ crystal, the bandwidth for negative refraction is about 0.57 MHz, and in this frequency range, electromagnetic wave may experience a negative refraction behavior. In the negative-refraction region, FOM (defined by n/k) has a maximum of 0.54 when frequency detuning is 0.45 MHz, where the complex refractive index is $-0.56 + 1.03i$.

However, the magnitude of negative refractive index is a little smaller and its bandwidth is also much narrower compared to negative refraction materials based on metallic periodic structures [35–37]. According to Eqs. (2) and (8), the amplitude and bandwidth of magnetic (electric) resonance are determined by dipole matrix element, atomic concentration and decay rate of levels. Sample with bigger matrix element and higher ion concentration is prone to possessing a bigger amplitude and wider bandwidth. In contrast, the effects of decay rate on them are opposite. For certain rare earth ions, dipole matrix element is fixed, whereas decay rate changes with temperature and concentration. If temperature is invariant and concentration changes in a small range, decay rate can also be treated as a constant and then atomic concentration is the dominant factor. Therefore, increasing the ratio of rare earth ions is an effective way to enhance the magnitude and bandwidth of negative refraction. In addition, if we refer to the absorption spectra of rare earth ions at room temperature, it is easily found that the FWHM usually reaches up to several nanometers due to phonon broadening and stark levels. As a result, the amplitude of electromagnetic resonance will decrease further and abnormal dielectric and magnetic response may disappear. In order to lower the effect of phonon, low-temperature environment is required.

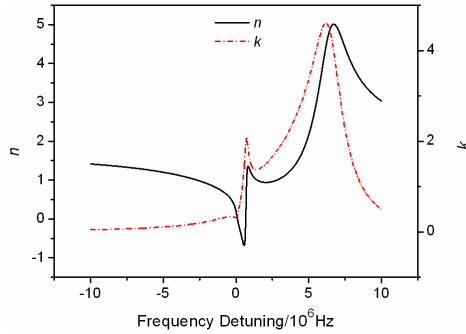


Figure 4. The optical constants v.s. frequency detuning. n and k denote the real part and imaginary part of refractive index, respectively.

4. CONCLUSIONS

In conclusion, we explored the magnetic and electric dipole transitions in rare earth ions doped crystals for realizing electromagnetic resonance and negative refraction at optical frequencies. Under the two-level approximation and weak field approximation, we analyzed the magnetic response and dielectric response in this system. It is found that negative permeability and permittivity can be attained near respective transition frequencies. By degenerating the two sets of levels, negative refraction can be achieved. As a typical example, the EM parameters of $(\text{Yb}_{0.02}\text{Sm}_{0.02}\text{Y}_{0.96})_3\text{Al}_5\text{O}_{12}$ crystal are calculated numerically. It is shown that the frequency range for negative refraction is about 0.57 MHz and the optimum refractive index is $-0.56 + 1.03i$. The simplicity of level model and free of strong controlled or driven field makes the scheme more practicable and applicable. What is more, the conditions of low temperature and high ion concentration may be adopted in order to get strong enough EM response in consideration of the phonon interference. It is believed that the proposed naturally occurring material would be a promising candidate material to realize magnetic response and negative refraction at optical frequencies.

ACKNOWLEDGMENT

This work was supported by the National Natural Science Foundation of China under Grant Nos. 90922025, 51032003, 50921061, and 51102148, and National High Technology Research and Development Program of China under Grant No. 2012AA030403.

REFERENCES

1. Viktor, G. V., "The electrodynamics of substances with simultaneously negative values of ε and μ ," *Sov. Phys. Uspekhi*, Vol. 10, 509–514, 1968.
2. Pendry, J. B., "Negative refraction makes a perfect lens," *Phys. Rev. Lett.*, Vol. 85, 3966–3969, 2000.
3. Grzegorzczuk, T. M., X. Chen, J. Pacheco, Jr., J. Chen, B. I. Wu, and J. A. Kong, "Reflection coefficients and Goos-Hänchen shifts in anisotropic and bianisotropic left-handed metamaterials," *Progress In Electromagnetics Research*, Vol. 51, 83–113, 2005.
4. Wongkasem, N., A. Akyurtlu, J. Li, A. Tibolt, Z. Kang, and W. D. Goodhue, "Novel broadband terahertz negative refractive index metamaterials: Analysis and experiment," *Progress In Electromagnetics Research*, Vol. 64, 205–218, 2006.
5. Schurig, D., J. J. Mock, B. J. Justice, S. A. Cummer, J. B. Pendry, A. F. Starr, and D. R. Smith, "Metamaterial electromagnetic cloak at microwave frequencies," *Science*, Vol. 314, 977–980, 2006.
6. Xi, S., H. Chen, B. I. Wu, and J. A. Kong, "Experimental confirmation of guidance properties using planar anisotropic left-handed metamaterial slabs based on S-ring resonators," *Progress In Electromagnetics Research*, Vol. 84, 279–287, 2008.
7. Pendry, J. B., A. J. Holden, D. J. Robbins, and W. J. Stewart, "Magnetism from conductors and enhanced nonlinear phenomena," *IEEE T. Microw. Theory.*, Vol. 47, 2075–2084, 1999.
8. Smith, D. R., W. J. Padilla, D. C. Vier, S. C. Nemat-Nasser, and S. Schultz, "Composite medium with simultaneously negative permeability and permittivity," *Phys. Rev. Lett.*, Vol. 84, 4184–4187, 2000.
9. Veselago, V. G. and E. E. Narimanov, "The left hand of brightness: Past, present and future of negative index materials," *Nat. Mater.*, Vol. 5, 759–762, 2006.
10. Valentine, J., S. Zhang, T. Zentgraf, E. Ulin-Avila, D. A. Genov, G. Bartal, and X. Zhang, "Three-dimensional optical metamaterial with a negative refractive index," *Nature*, Vol. 455, 376–332, 2008.
11. Shalaev, V. M., "Optical negative-index metamaterials," *Nat. Photon.*, Vol. 1, 41–48, 2007.
12. Liu, N., H. Guo, L. Fu, S. Kaiser, H. Schweizer, and H. Giessen, "Three-dimensional photonic metamaterials at optical frequencies," *Nat. Mater.*, Vol. 7, 31–37, 2008.

13. Krowne, C. M., "The road to quantum level negative index metamaterials," *Waves Random Complex*, Vol. 20, 223–250, 2010.
14. Shen, J. Q., Z. C. Ruan, and S. L. He, "How to realize a negative refractive index material at the atomic level in an optical frequency range," *J. Zhejiang Univ.-Sc. A*, Vol. 5, 1322–1326, 2004.
15. Oktel, M. Ö. and Ö. E. Müstecaplıoğlu, "Electromagnetically induced left-handedness in a dense gas of three-level atoms," *Phys. Rev. A*, Vol. 70, 053806, 2004.
16. Shen, J. Q., "Gain-assisted negative refractive index in a quantum coherent medium," *Progress In Electromagnetics Research*, Vol. 133, 37–51, 2013.
17. Kussow, A. G. and A. Akyurtlu, "Negative refraction index in the magnetic semiconductor $\text{In}_{2-x}\text{Cr}_x\text{O}_3$: Theoretical analysis," *Phys. Rev. B*, Vol. 78, 205202, 2008.
18. Kussow, A. G. and A. Akyurtlu, "Electromagnetically induced negative refractive index in doped semiconductors at optical frequencies," *Int. J. Mod Phys B*, Vol. 25, 347–364, 2011.
19. Wybourne, B. G., *Spectroscopic Properties of Rare Earths*, John Wiley & Sons, Inc., New York, 1965.
20. Gschneidner, Jr., K. A. and L. Eyring, *Handbook on the Physics and Chemistry of Rare Earths*, Vol. 5, North Holland Publishing Company, Amsterdam, 1982.
21. Thommen, Q. and P. Mandel, "Left-handed properties of erbium-doped crystals," *Opt. Lett.*, Vol. 31, 1803–1805, 2006.
22. Liu, C. X., J. S. Zhang, J. Y. Liu, and G. Jin, "The electromagnetically induced negative refractive index in the Er^{3+} : YAlO_3 crystal," *J. Phys. B: At., Mol. Opt. Phys.*, Vol. 42, 095402, 2009.
23. Scully, M. O. and M. S. Zubairy, *Quantum Optics*, Cambridge University Press & Beijing World Publishing Corporation, Cambridge, 2009.
24. Krowne, C. M., "Multi-species two-level atomic media displaying electromagnetic left handedness," *Phys. Lett. A*, Vol. 372, 2304–2310, 2008.
25. Zare, R. N., *Angular Momentum: Understanding Spatial Aspects in Chemistry and Physics*, Wiley, New York, 1988.
26. Wu, C. T., Y. L. Ju, Z. G. Wang, Q. Wang, C. W. Song, and Y. Z. Wang, "Diode-pumped single frequency $\text{Tm} : \text{YAG}$ laser at room temperature," *Laser Phys. Lett.*, Vol. 5, 793–796, 2008.
27. Lacovara, P., H. K. Choi, C. A. Wang, R. L. Aggarwal, and T. Y. Fan, "Room-temperature diode-pumped $\text{Yb} : \text{YAG}$ laser,"

- Opt. Lett.*, Vol. 16, 1089–1091, 1991.
28. Judd, B. R., “Optical absorption intensities of rare-earth ions,” *Phys. Rev.*, Vol. 127, 750–761, 1962.
 29. Ofelt, G. S., “Intensities of crystal spectra of rare-earth ions,” *J. Chem. Phys.*, Vol. 37, 511–520, 1962.
 30. Fu, X. J., Y. D. Xu, and J. Zhou, “Abnormal dielectric response in an optical range based on electronic transition in rare-earth-ion-doped crystals,” *Chin. Phys. Lett.*, Vol. 29, 027805, 2012.
 31. Jackson, J. D., *Classical Electrodynamics*, Wiley, New York, 1999.
 32. Kaczkan, M., Z. Frukacz, and M. Malinowski, “Infrared-to-visible wavelength upconversion in Sm^{3+} -activated YAG crystals,” *J. Alloy. Compd.*, Vol. 323–324, 736–739, 2001.
 33. Malinowski, M., R. Wolski, Z. Frukacz, T. Lukasiewicz, and Z. Luczynski, “Spectroscopic studies of YAG: Sm^{3+} crystals,” *J. Appl. Spectrosc.*, Vol. 62, 840–843, 1995.
 34. Palik, E. D., *Handbook of Optical Constants of Solids*, Academic Press, San Diego, CA, 1998.
 35. Li, J., F.-Q. Yang, and J. Dong, “Design and simulation of L-shaped chiral negative refractive index structure,” *Progress In Electromagnetics Research*, Vol. 116, 395–408, 2011.
 36. Aslam, M. I. and D. O. Gueney, “On negative index metamaterial spacers and their unusual optical properties,” *Progress In Electromagnetics Research B*, Vol. 47, 203–217, 2013.
 37. Guo, J., Y. Xiang, X. Dai, and S. Wen, “Enhanced nonlinearities in double-fishnet negative-index photonic metamaterials,” *Progress In Electromagnetics Research*, Vol. 136, 269–282, 2013.